Optimizing immersion media refractive index improves optical trapping by compensating spherical aberrations

S. Nader S. Reihani[1,2,*] and Lene B. Oddershede[1,3]

[1]*Niels Bohr Institute, Blegdamsvej 17, 2100 Copenhagen, Denmark*
[2]*Institute for Advanced Studies in Basic Sciences (IASBS), Zanjan 45195-1159, Iran*
[3] *E-mail: oddershede@nbi.dk*
**Corresponding author: reihani@nbi.dk*

Received January 9, 2007; revised May 8, 2007; accepted May 9, 2007;
posted May 18, 2007 (Doc. ID 82291); published July 3, 2007

The efficiency of an optical trap is limited by its axial strength. Light focused by oil-immersion objectives provides stronger traps but suffers from spherical aberrations, thus restricting the axial stability and working distance. By changing the refractive index of the immersion media we compensate spherical aberrations and measure axial trapping strengths at least twice as large as previously reported. Moreover, the spherical aberrations can be compensated at any desired depth. The improved trapping efficiency implies significantly less heating of the particles, thus diminishing previously published concerns about using gold nanoparticles as handles for optical manipulation. © 2007 Optical Society of America

OCIS codes: 140.7010, 220.1000, 170.1790.

Over the past decade optical tweezers have been used widely as a tool for micromanipulation [1]. Also, metallic nanoparticles can be optically trapped [2], and these are predicted to have potential as *in vivo* handles in biological specimens if the laser-heating effects [3] can be minimized. Oil-immersion objectives can have a higher numerical aperture (NA) than water immersion ones and are therefore favorable to use for microscopy and optical trapping. However, a common problem with using oil-immersion objective lenses is the presence of the spherical aberrations (SAs) owing to the mismatch in the refractive indices of the immersion and specimen media that widen the focal volume progressively with trapping depth. Several methods have been suggested to improve spherical aberrations, e.g., deformable mirrors in multiphoton scanning microscopy [4] and in optical tweezing [5]. Implementing deformable mirrors is fairly cumbersome and expensive in comparison with the methods here presented. Other methods to correct for SAs include changing the tube length [6,7].

The SAs appear as a phase in the intensity point-spread function [8] (IPSF), and the total SA is a sum of different contributions, all of which depend on the wavelength of the laser light:

$$SA_{total} = SA_{tube} + SA_{obj} + SA_{im/cov} + SA_{cov/sample}, \tag{1}$$

where SA_{tube} is a contribution that stems from the tube length of the particular microscope. SA_{obj} is the contribution from the lenses in the objective. Typically, the objective lenses are adjusted to minimize the SA at visible wavelengths but are not optimized for infrared laser light. $SA_{im/cov}$ and $SA_{cov/sample}$ denote the spherical abberations introduced by the possible mismatch in refractive indices of the immersion media of the objective, the cover glass, and the media within the sample, respectively. Both these contributions depend on the distance traveled by the light within the various media. Minimizing SA_{total} at any given depth produces the most focused laser beam.

The idea is to modify the third term in Eq. (1), $SA_{im/cov}$, such that it optimally cancels the SA introduced by the other terms. The depth at which optimal compensation occurs can be adjusted by changing refractive index of the immersion oil.

Our optical tweezer setup [9] is based on a Nd:YVO_4 laser with wavelength 1064 nm and is implemented in an inverted Leica microscope with a quadrant photodiode back-focal-plane detection scheme. The objective is from Leica (HCX PL Apo, 63×, NA=1.32, ∞, 0.17). The position time series of the trapped beads were acquired by using a custom-made LabView program and analyzed by using a Matlab-based power spectrum analysis program [10]. The trap constitutes a harmonic potential and is characterized by a spring constant, k, which is related to the corner frequency f_c by $k=2\pi\gamma f_c$, γ being the drag coefficient of the trapped bead that is far from the glass surface.

To perform the most accurate measurements of the spring constant in the axial direction the NA of the condenser is set to 0.4 [11]. For measurements of bead positions in the lateral direction the condenser aperture was fully opened.

For an objective satisfying the sine condition and illuminated with a linearly polarized Gaussian laser beam, the effect of the SA on the three-dimensional (3D) IPSF in the second medium can be accounted for by a phase factor [8]. In the case where the SAs are caused by a mismatch between refractive indices of two media, the phase factor at depth d_w in the second medium is given by [8]

$$\psi(\theta_1, \theta_2, -d_w) = -k_0 d_w (n_1 \cos\theta_1 - n_2 \cos\theta_2), \tag{2}$$

where θ_1, θ_2, k_0, and d_w are incident angle in first medium, refracted angle in second medium, wavenum-

0146-9592/07/141998-3/$15.00

ber in vacuum, and the nominal trapping depth, i.e., the distance traveled by the objective, respectively. From here d_w will simply be called the depth. Figure 1 shows these values as well as a schematic diagram of the optical path for marginal rays. d'_w is the actual trapping depth, which is unknown but approximately 20% off d_w. When the immersion oil and the cover glass are index matched, which occurs for conventional immersion oils (dotted line in Fig. 1), θ_1 and θ_2 can be easily calculated as 60.4° and 83°, respectively ($\mathrm{NA}=1.32=n_1 \sin \theta_1$ and $n_1 \sin \theta_1 = n_2 \sin \theta_2$ with $n_1 = 1.518$ and $n_2 = 1.33$). In this case the only component of the phase factor arising from the glass–water interface can be written as $\psi_{gw} = -0.59\, k_0 d_w$. In the case where the immersion oil and the glass are not index matched, this introduces an additional phase component that can be calculated in same manner. Increasing immersion oil index of refraction by $\triangle n = 0.01$ implies $\theta_0 = 59.7°$ (see Fig. 1 for a definition of θ_0). Thus, the component of the phase factor arising from the oil–glass interface can be written as $\psi_{og} = 0.021\, k_0 d_o$, where d_o is the thickness of the oil layer. We measured this thickness to be $115 \pm 15\ \mu$m by measuring the travel of the objective from the focus of the inside surface of the coverslip until the objective hit the sample. The optimal depth for optical trapping is the depth where the various sources of spherical abberations cancel, e.g., where $\psi_{gw} + \psi_{og} = 0$, which gives a change in optimal trapping depth of $\triangle d_w = 4.1 \pm 0.5\ \mu$m; an increase of 0.01 in the refractive index of the immersion oil moves the optimal trapping depth $(4.1 \pm 0.5)\ \mu$m deeper into the sample. If this method is combined, e.g., with changing tube length [7], then the optimal trapping depth can be changed continuously.

To experimentally show how the optimal trapping depth depends on the index of refraction of the immersion oil, we performed a series of experiments using immersion oils with refractive indices ranging from 1.51 to 1.57 (Cargille, refractive index liquids set A). For each immersion oil the axial spring constant was measured at different trapping depths (Fig. 2). Each data point in Fig. 2 is representative of 25 measurements (5 different beads, 5 measurements for each bead). The experiment was performed using a single immersion oil at a time. Between experiments with different immersion oils the objective was carefully cleaned and the chamber was replaced. The error bars in the spring constants are less than 5% and are not shown. Figure 2 illustrates that: (1) Using the conventional oil ($n = 1.518$, Leica) provides a maximum trapping strength of only ~1/3 of the maximum strength possible. For trapping close to the cover glass an immersion oil with refractive index 1.53–1.54 apparently provides the strongest trap. For immersion oils with refractive indices below ~1.53 the peak of the curve lies outside the measurable region at negative trapping depths. (2) The depth at which the optical trap is strongest in the axial direction increases with the refractive index of the immersion oil. In accordance with the calculation above, the experiments show that an 0.01 increment in the refractive index gives rise to a shift of $\simeq 3\ \mu$m in the optimal trapping depth. (3) The graphs corresponding to different immersion oil refractive indices have nearly the same value of maximum spring constant and appear as horizontal shifts of each other. Hence, if one wishes to perform an experiment at a given depth within the sample, it is important to choose the correct immersion oil to have maximum trapping efficiency at that particular depth.

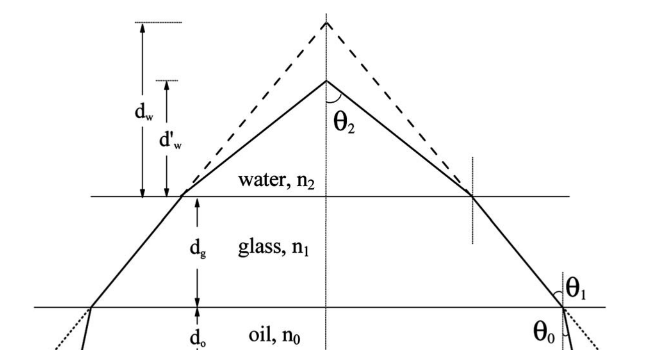

Fig. 1. Schematic drawing of marginal rays.

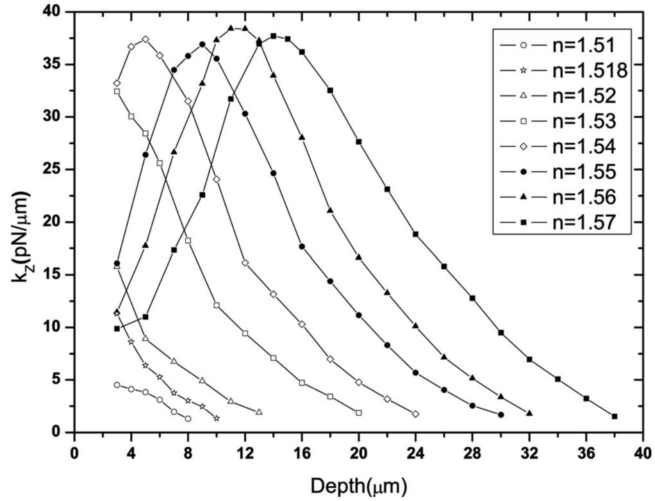

Fig. 2. Axial spring constant as a function of trapping depth for PS beads with a diameter of 1.01 μm using immersion oils with different refractive indices. Laser power at the sample, 37 mW.

To further investigate the quality of the optical trap we measured its performance in trapping submicron particles. Figure 3 shows the result of 3D measurements of trapping strength versus laser power at a trapping depth of $5 \pm 0.5\ \mu$m for 0.33, 0.49, 0.8, and 1.01 μm polystyrene (PS) beads using an immersion oil with $n = 1.54$. The laser power was measured at the exit of the objective. Figure 3 shows that: (1) all components of the spring constant increase linearly with laser power, which is a fundamental property of an optical trap. From the slopes the trapping efficiency, Q_{max}, can be calculated; $Q_{max} = kac/Pn$, where k, a, c, P, and n are spring constant, radius of the trapped bead, speed of light, laser power at the sample, and the refractive index of the immersion medium, respectively. For a 0.8 μm bead $Q_{max,z} = 0.09$, which to our knowledge is more than twice the

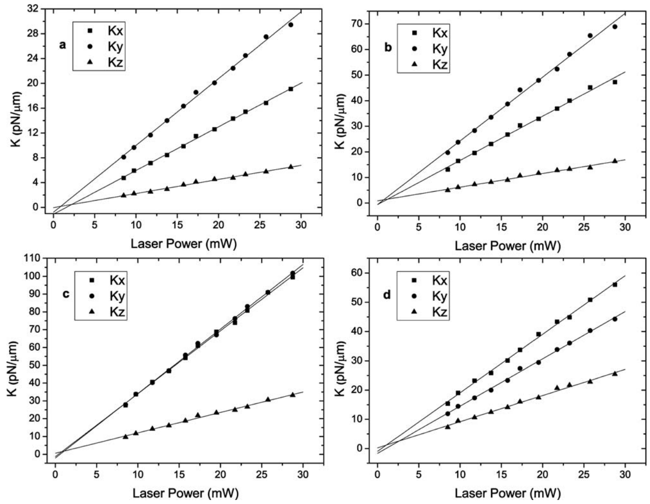

Fig. 3. Trapping strength as a function of laser power measured at the sample for PS beads with diameters of a, 0.33; b, 0.49; c, 0.8; and d, 1.01 μm. Each data point is an average from 5 measurements.

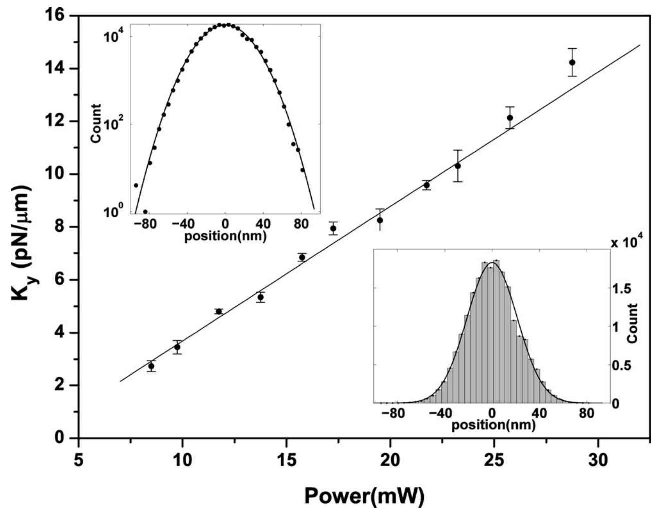

Fig. 4. Spring constant in the y direction as a function of laser power while trapping 100 nm gold nanoparticles. Insets show position distributions on linear (right) and semilog (left) scales, respectively. Laser power at the sample, 26 mW.

highest reported axial efficiency [12]. (2) The ratio of the lateral to axial trapping strength is bead-size dependent and about two times lower than the value reported in [12], which shows that the current method improves the axial efficiency more than the lateral one. (3) The anisotropy of the spring constants describing the trap in the orthogonal directions, k_x and k_y, is size dependent, and it changes sign at a bead diameter of $\sim 0.8\ \mu$m in accordance with the results in [12].

A problem associated with optical trapping of metal nanoparticles is heating caused by absorption [3]. Increasing the efficiency of the optical trap allows for considerable forces to be exerted on the metallic particles without causing significant heating. This is illustrated in Fig. 4, which shows how the lateral trapping strength for gold nanoparticles with 100 nm diameter (BB International) varies with the laser power under optimal trapping conditions ($n=1.54$, trapping depth$=5\ \mu$m). The optical trap is very efficient: the laser power producing a trapping strength of 12 pN/μm was ~ 25 mW, which is more than 24 and 8 times better than the equivalent values reported in [2,3], respectively. When the heating ratio of 266 deg/W reported in [3] was used, this trap gave rise to a temperature increase of less than 7°. Position histograms for a laser power of 26 mW (see insets in Fig. 4) show that for displacements as large as 80 nm the potential remains harmonic, giving rise to forces in the pico-Newton regime.

It is important for the performance of an optical trap that the index of refraction of the immersion oil is chosen to cancel the spherical abberations introduced by other means in the optical path. Optical trapping can be efficiently performed hundreds of micrometers inside an aqueous chamber, even using oil-immersion objectives. An increment (decrement) of 0.01 in the refractive index of the immersion oil gives rise to an increase (decrease) of about 3–4 μm in optimal trapping depth. Further, the trapping efficiency here reported is, to our knowledge, at least twice as strong as previously reported. Also, we have shown that gold nanoparticles can be trapped using eight times less laser power than previously reported [3], thus significantly reducing the associated heating associated with the optical trapping.

The authors acknowledge comments from P. M. Hansen and financial support from the Villum Kann Rasmussen Foundation.

References

1. A. Ashkin, J. M. Dziedzic, and T. Yamane, Nature **330**, 769 (1987).
2. P. M. Hansen, V. K. Bhatia, and L. Oddershede, Nano Lett. **5**, 1937 (2005).
3. Y. Seol, A. E. Carpenter, and T. T. Perkins, Opt. Lett. **31**, 2429 (2006).
4. L. Sherman, J. Y. Ye, O. Albert, and T. B. Norris, J. Microsc. **206**, 65 (2002).
5. T. Ota, T. Sugiura, S. Kawata, M. J. Booth, M. A. A. Neil, R. Juskaitis, and T. Wilson, Jpn. J. Appl. Phys., Part 1 **42**, L701 (2003).
6. S. N. S. Reihani, H. R. Khalesifard, and R. Golestanian, Opt. Commun. **259**, 204 (2006).
7. S. N. S. Reihani, M. A. Charsooghi, H. R. Khalesifard, and R. Golestanian, Opt. Lett. **31**, 766 (2006).
8. P. C. Ke and M. Gu, J. Mod. Opt. **45**, 2159 (1998).
9. L. Oddershede, S. Grego, S. Nørrelykke, and K. Berg-Sørensen, Probe Microsc. **2**, 129 (2001).
10. K. Berg-Sørensen and H. Flyvbjerg, Rev. Sci. Instrum. **75**, 594 (2004).
11. J. K. Dreyer, K. Berg-Sørensen, and L. Oddershede, Appl. Opt. **43**, 1991 (2004).
12. A. Rohrbach, Phys. Rev. Lett. **95**, 168102 (2005).